≪ Research Paper ≫

Injectable Apatite for the Sequestration of Sr-90 in Groundwater

Sung-Wook Jeen[1]* · Yunjung Hyun[2]

[1]*Department of Earth and Environmental Sciences & The Earth and Environmental Science System Research Center, Chonbuk National University, Korea*
[2]*Korea Environment Institute, Korea*

ABSTRACT

Laboratory column experiments were conducted to evaluate the feasibility of injectable apatite method for the sequestration of Sr-90 in groundwater. The columns were tested to evaluate the rate of citrate biodegradation, the amounts of apatite formed, and the treatability of strontium by the sediment and apatite. The results showed the decreases in citrate, calcium, and phosphate concentrations and the increases in alkalinity and citrate degradation products (acetate and formate) in the columns, suggesting that the citrate degradation and formation of calcium phosphate are occurring. Although the calcium and phosphate were not completely consumed within the columns, some amounts of apatite were formed and it showed an ability to treat strontium in groundwater. This study provides a fundamental understanding of reaction mechanisms for the injectable apatite sequestration method for Sr-90 removal.

Key words : Apatite, Column experiment, Groundwater, Sequestration, Strontium-90

1. Introduction

Sr-90 is one of the most problematic radioactive contaminants in groundwater at many nuclear sites. Although Sr-90 is naturally retarded by sorption onto mineral surfaces, it is sufficiently mobile and long-lived to require treatment in many hydrogeological settings (Killey and Munch, 1987; Yin et al., 2014).

Apatite $[Ca_{10}(PO_4)_6(OH)_2]$ is a natural calcium phosphate mineral and can sequester elements into its molecular structure via isomorphic substitution, whereby elements of similar physical and chemical characteristics replace calcium, phosphate, or hydroxide in the hexagonal crystal structure (Hughes et al., 1989; Spence and Shi, 2005). This mineral can be used to sequester radionuclides such as Sr-90 because chemical behaviors of stable and radioactive strontium are essentially same. Using apatite for the treatment of the radionuclide Sr-90 in subsurface environments involves proper emplacement methods such as conventional trench-and-fill permeable reactive barriers (PRBs) (e.g., Seneca and Rabideau, 2013). One innovative method of emplacing apatite in the subsurface sediments is to inject an aqueous solution containing Ca-citrate-phosphate complex (Moore et al., 2004). Emplacement of apatite precipitate by solution injection has significant advantages over other apatite emplacement methods (e.g., minimal disturbance of the subsurface). This method extends the PRB concept to sites where groundwater contaminants are too deep or where site conditions otherwise preclude the application of more traditional trench-emplaced barriers (Vermeul et al., 2014).

Mechanisms are needed for delaying the formation of insoluble compounds until the source areas are permeated by the calcium and phosphate ions, which then form insoluble apatite. Citrate is needed to keep calcium and phosphate in solution long enough (days) to be injected into the subsurface. Relatively slow biodegradation of the Ca-citrate complex allows sufficient time for injection and transport of the reagents to the areas of the aquifer where treatment is required (Vermeul et al., 2014). As Ca-citrate is degraded by naturally-occurring microbes, the free calcium and phosphate combine to form amorphous apatite. Apatite incorporates some Sr-90 during initial precipitation and, in

addition, it slowly incorporates Sr-90 by solid phase substitution for calcium. Strontium substitution occurs because strontium-apatite is thermodynamically more stable than calcium-apatite (Verbeeck et al., 1977). Once substituted, Sr-90 is immobilized as a solid and is radioactively decayed to Y-90 and then to Zr-90 (Thompson et al., 2009).

The injectable apatite sequestration method has primarily been tested by researchers at the Hanford site (Williams et al., 2008; Thompson et al., 2009; Szecsody et al., 2010; Fritz et al., 2011). While the idea is geochemically and theoretically sound, this method is still immature (i.e., few publications are available in the public domain) and there are knowledge gaps that have to be filled before it can be applied to the field sites. In this study, column experiments were conducted to evaluate the feasibility of apatite sequestration of Sr-90 in groundwater. Particularly, the rates of citrate degradation, the amounts of apatite formed, and the removal of strontium by the apatite precipitates and sediments were evaluated to provide an understanding of the underlying reaction mechanisms for the injectable apatite sequestration method.

2. Materials and Methods

2.1. Columns

Two columns (columns 1 and 2) were manufactured, and each column consisted of a 40 cm long clear Plexiglas™ tube with an internal diameter of 7.62 cm. Ten sampling ports were located at 2.5, 5, 7.5, 10, 12.5, 15, 20, 25, 30, and 35 cm from the influent end. Columns were packed with the sediment collected from a site in Chalk River, Ontario, Canada to evaluate the potential possibility of

using the method in the site. The grain size analysis showed that the sediment can be classified as fine to medium sand. Sediment was packed after sieving with #10 sieve (2 mm); however, it was not dried to preserve the native microorganisms in the sediment. The porosity was determined from the volume of each column, the total mass of sediment added, and the column weight measured after saturation of the column with de-ionized water. Sediment water contents were also measured (3.68% for column 1 and 3.94% for column 2), and were compensated for the calculations of mass of dry sediment and pore volume (PV). Column characteristics are summarized in Table 1. Two columns were operated with a series of different operational conditions to evaluate the following processes (Table 2): biodegradation of citrate and its degradation products, formation of calcium phosphate (apatite), and adsorption/incorporation of strontium into apatite/sediment.

2.2. Source Solutions

A mixed solution of sodium citrate, calcium chloride, disodium phosphate, monosodium phosphate, and diammonium phosphate was used for preparing the source solution. To minimize citrate degradation in the source bottles, fresh solution was prepared every 3-4 days. Also, the source

Table 1. Column properties

	Column 1	Column 2
Dry soil mass (g)	2733.62	2722.70
Pore volume (PV) (cm³)	660.29	682.90
Bulk density (g/cm³)	1.50	1.49
Porosity	0.36	0.37
Sediment : Solution ratio	4.14 : 1	3.99 : 1

Table 2. Operation history for the column experiments

		Source composition	Flow velocity	Operation period (days)
Column 1		10 mM sodium citrate, 4 mM calcium chloride, 2 mM disodium phosphate, 0.3 mM monosodium phosphate, 0.15 mM diammonium phosphate	1 mL/min (2.2 PV/day)	75
Column 2	Phase I	50 mM sodium citrate, 20 mM calcium chloride, 10 mM disodium phosphate, 1.5 mM monosodium phosphate, 0.5 mM diammonium phosphate	1 mL/min (2.1 PV/day)	16
	Phase II	5 mM sodium citrate, 2 mM calcium chloride, 1 mM disodium phosphate, 0.15 mM monosodium phosphate, 0.05 mM diammonium phosphate	1 mL/min (2.1 PV/day)[a]	33
	Phase III	Groundwater spiked with 1 mg/L Sr	1 mL/min (2.1 PV/day)	10

[a] Except for 1.85 mL/min (3.9 PV/day) between day 26 to day 27

Table 3. Chemical composition of the uncontaminated groundwater used in phase III of column 2

Component	Concentration
pH	6.00
Ba^{2+} (mg/L)	0.013
Ca^{2+} (mg/L)	5.68
Fe^{2+} (mg/L)	0.04
K^+ (mg/L)	1.21
Mg^{2+} (mg/L)	1.23
Mn^{2+} (mg/L)	0.009
Na^+ (mg/L)	9.97
Cl^- (mg/L)	19.7
CO_3^{2-} (mg/L)	7.64
NO_3^- (mg/L)	0.60
SO_4^{2-} (mg/L)	7.35

bottles and columns were wrapped with aluminum foils to prevent photodegradation of the citrate. The source solution was pumped through the columns using a peristaltic pump (Ismatec 78001-02) at desired flow rates (1 mL/min for column 1 and most of time for column 2 and 1.85 mL/min between day 26 to day 27 for phase II of column 2) (Table 2). In phase III of column 2, the source solution was switched from the Ca-citrate-phosphate solution to the uncontaminated groundwater (Table 3), obtained from the same site where the sediment was collected, after spiked with 1 mg/L Sr (stable Sr as a surrogate for Sr-90 (Rabideau et al., 2005; Chang et al., 2011)) (Table 2). All source solutions were supplied to the columns as continuous injection systems.

2.3. Sampling and Analysis

Water samples were collected along the lengths of the columns through the sampling ports. Samples were collected with a glass syringe from top to bottom under the naturally-flowing condition, i.e., no suction was induced. The pH probe (Beckman pH electrode 511275-AB) was calibrated with the standard 4.0, 7.0, and 10.0 pH buffer solutions, and the pHs were measured with the Beckman PHI 265 pH/Temp/mV meter. Alkalinity was measured using a HACH digital titrator with 1.6 N sulphuric acid and bromo-cresol green/methyl red indicator. For analyses of anions and cations, samples were filtered using a 0.22 μm filter (cellulose acetate sterile filters) to filter bacteria possibly present in the

water. Anions were analyzed with ion chromatography (IC). Samples for cation analysis were acidified with ultra-trace grade nitric acid and analyzed with inductively coupled plasma-atomic emission spectroscopy (ICP-AES).

At the termination of the column experiments, the sediment inside column 1 was sectioned and dried in a fume hood for several days. A subsample collected in 0-2.5 cm from the influent end, as well as the raw sediment, was analyzed for cation exchange capacity (CEC), using the barium chloride-triethanolamine method (Mehlich, 1938), to determine whether or not the apatite formed increases the CEC.

3. Results and Discussion

3.1. Geochemical Changes

3.1.1. Column 1

The composition of the source solution for column 1 was based on the stoichiometric precipitation of apatite (4 mM of Ca : 2.4 mM of PO_4) with enough citrate (10 mM) to complex with calcium. Fig. 1 shows the profiles of citrate, carbonate, acetate, formate, Ca, and P measured in different weeks for column 1. The citrate was degraded rapidly within 5-10 cm from the influent end of the column (Fig. 1a). Increase in carbonate concentration was also observed (Fig. 1b), consistent with the increase in alkalinity (not shown). Szecsody et al. (2007) showed that anaerobic citrate degradation produces acetate and formate, while in aerobic systems citrate is completely mineralized to CO_2. The detection of acetate and formate (Fig. 1c and d) thus suggests that although the experiments were performed under initially aerobic condition, anaerobic conditions developed quickly within the column. The Ca and P concentrations were decreasing only for the first week (Fig. 1e and f) (phosphate concentrations were consistent with P concentrations). At later sampling occasions, the concentrations of Ca and P were slightly increasing within the column, possibly due to re-dissolution of calcium phosphate previously formed. The CEC value measured for the column 1 sample at the termination of the experiments was 2.04 meq/100 g, while the value for the raw sediment was 1.26 meq/100 g. This indicates that the apatite precipitated in the sediment increased the CEC.
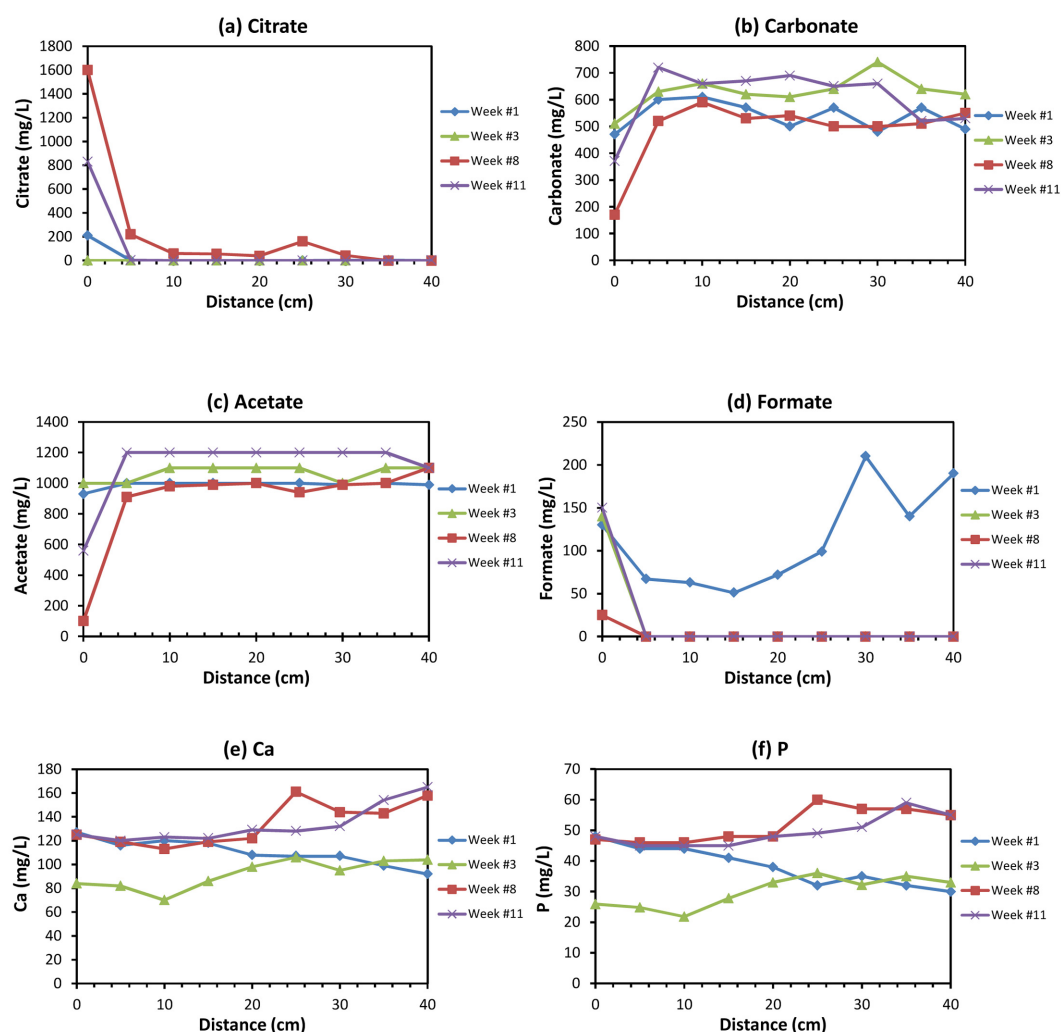
Fig. 1. The concentration profiles of column 1 measured in different weeks: (a) citrate, (b) carbonate, (c) acetate, (d) formate, (e) Ca, and (f) P.

According to Szecsody et al. (2007), citric acid is utilized by organic systems, where the citrate is converted to C6, C5, and C4 organic acids producing CO_2 and H^+, and then cycled from oxaloacetic acid (C4) to citric acid. Citrate can also be further degraded to acetic acid (C2), formaldehyde, formic acid (C1), and CO_2. Degradation of citrate and formation of apatite will lead to decreases in pH, citrate, calcium, and phosphate concentrations, and increase in alkalinity. The results in this study showed that citrate was degraded, forming acetate and formate. Alkalinity (bicarbonate/carbonate) was increasing along the length of the column, while pH was slightly decreasing. Also, calcium and phosphate (and P) were decreasing, indicating that calcium phosphate is formed within the column. These results

suggest that the fundamental geochemical reactions for the in situ apatite sequestration were occurring in the column. However, this observation was applicable only to the first week of the experiments in this column. At later times, there were little changes in the calcium and phosphate concentrations in the first half of the column and even slight increases in the second half were observed, whereas the citrate was still degraded near the influent end. It is speculated that the initially-formed calcium phosphate solid may be dissolving due to the changes in the geochemical conditions.

3.1.2. Column 2 - phase I

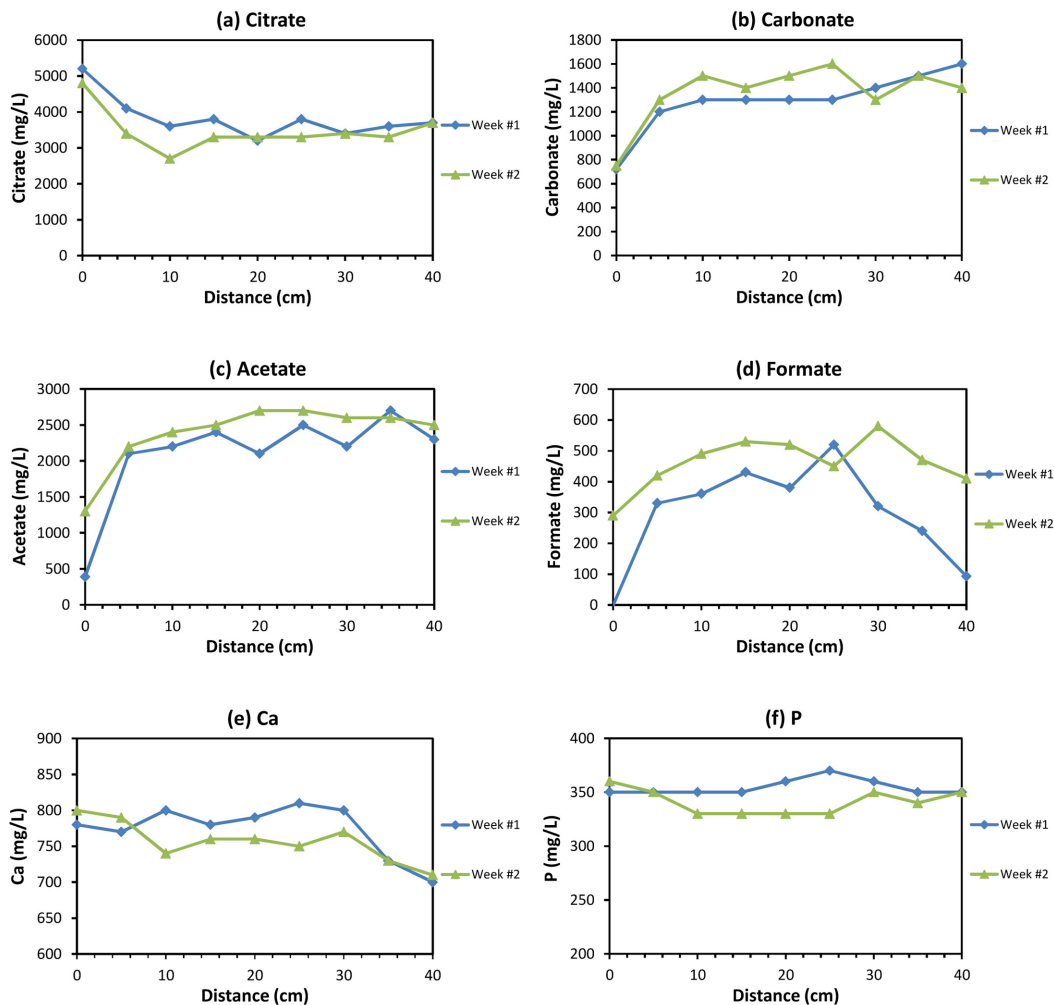Fig. 2 shows the profiles of citrate, carbonate, acetate,

Fig. 2. The concentration profiles of column 2 measured in phase I of the operation periods: (a) citrate, (b) carbonate, (c) acetate, (d) formate, (e) Ca, and (f) P.

formate, Ca, and P measured in phase I of column 2, in which higher concentrations of citrate, calcium, and phosphate were supplied compared to column 1. The results showed that the citrate was degraded to about half initially and remained constant in the remaining portion of the column (Fig. 2a). The other geochemical measurements were rather similar to column 1: slight decrease in pH and increase in alkalinity (not shown), increases in carbonate, acetate, and formate (Fig. 2b to d). Interestingly, formate initially increased and then decreased after about half distance of the column, indicating that formate generated from the citrate degradation is also degraded by subsequent biodegradation processes (Szecsody et al., 2007). The changes in the phosphate concentrations were not significant, while the calcium concentration decreased by 80-90 mg/L within the column (Fig. 2e

and f). Although the purpose of phase I of column 2 was to precipitate a larger amount of apatite within shorter periods of time (concentrations were 5 times higher than column 1), the results suggested that the calcium and phosphate were not consumed as intended, probably due to complexing of calcium with citrate degradation products or slow kinetics of apatite precipitation.

3.1.3. Column 2 - phase II

The composition of the source solution for phase II was 10 times diluted compared to that for phase I (Table 2). Fig. 3 shows the profiles of citrate, Ca, P, and pH measured in phase II. The first profile sampling was conducted with the normal flow rate (1 mL/min; 2.2 PV/day), but the second sampling was conducted with a higher flow rate (2 mL/min)
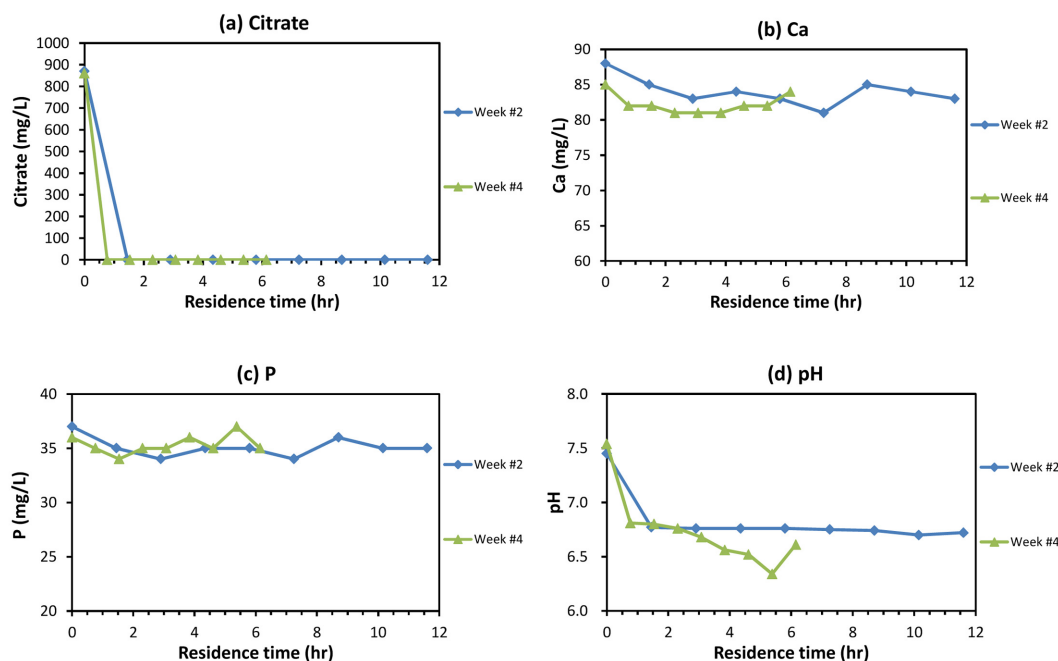
Fig. 3. The concentration profiles of column 2 measured in phase II of the operation periods: (a) citrate, (b) Ca, (c) P, and (d) pH.

to assess the potential differences in reaction rates with different velocities. Concentrations were thus plotted against residence time to compare the two sampling occasions with different flow rates.

In phase II, although the citrate was fast degraded (Fig. 3a), there was only little consumption of Ca and phosphate within the column, as seen in the concentrations of Ca and P (Fig. 3b and c). This indicates that formation of apatite is limited in this operational condition. For the column velocities employed, i.e., 0.8 m/day to 1.6 m/day, the difference in flow velocity does not appear to affect chemical reactions. The two profiles were similar in that the pH was decreasing (Fig. 3d) and the alkalinity and the concentrations of carbonate, acetate, and formate were increasing (not shown).

3.1.4. Column 2 - phase III

The purpose of phase III was to evaluate the treatability of Sr by the sediment and apatite formed during phases I and II. The source solution was switched from the Ca-citrate-phosphate solution to the site groundwater spiked with 1 mg/L Sr (Table 2). This is the expected condition that groundwater passes through the in situ apatite PRB after injection of Ca-citrate--phosphate solution (after citrate degradation is completed and apatite is formed).

As seen in Fig. 4a, the Sr was completely treated within 5 cm from the influent end for the first week and within 15 cm from the influent end for the second week. The migration of the Sr treatment front may be due to either exhaustion of sorption capacity of sediment/apatite near the influent end or dissolution of amorphous calcium phosphate that was previously formed. The concentrations of Ca and P (Fig. 4b and c) partially support the possibility that amorphous calcium phosphate is dissolving. It is also interesting to note that the concentrations of Ca and P were increasing but then decreasing toward the effluent end of the column, suggesting that calcium phosphate is re-precipitating in the portion close to the effluent end. The concentrations of Mg (Fig. 4d) were decreasing, suggesting precipitation of Mg-containing minerals and/or ion-exchange reactions between Mg and Ca (or other cations).

3.2. Reaction Mechanisms and Implications to Field Applications

Citrate degradation rates were calculated based on the changes in the citrate concentrations versus residence time, using a pseudo-first order kinetic model. The calculated citrate degradation rates were 1.108, 0.013, and 2.134 hr^{-1} for column 1, column 2 - phase I, and column 2 - phase II,
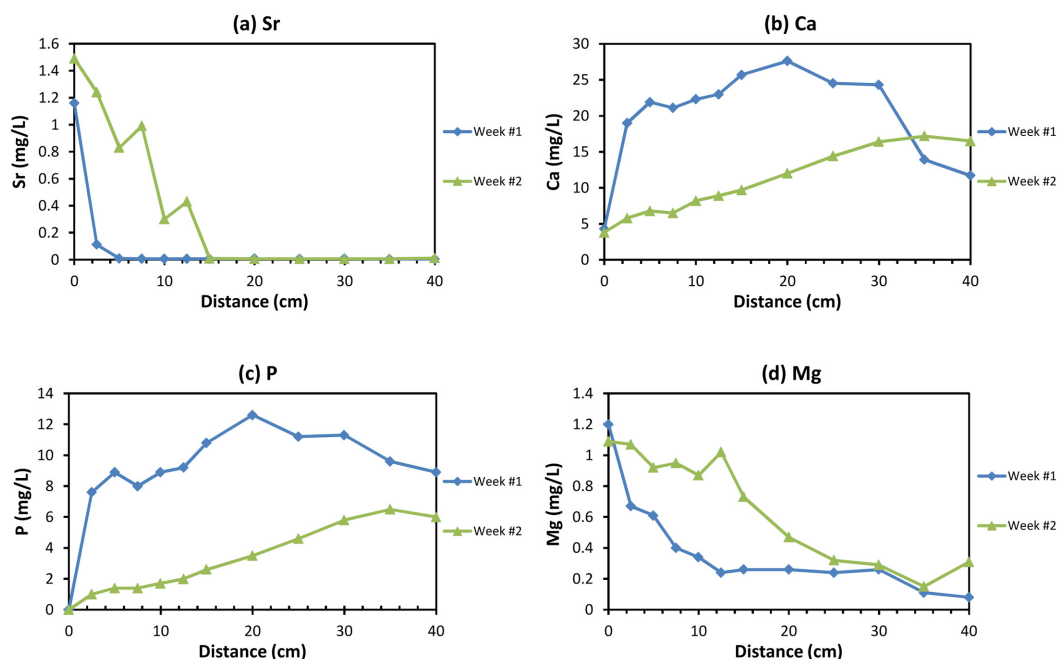
Fig. 4. The concentration profiles of column 2 measured in phase III of the operation periods: (a) Sr, (b) Ca, (c) P, and (d) Mg.

respectively. These correspond to half-lives of 0.626, 53.319, and 0.325 hr, respectively. The laboratory citrate degradation rates at the Hanford site were 0.025 and 0.013 hr^{-1} for citrate concentrations of 10 and 50 mM, respectively (Szecsody et al., 2007). The citrate degradation rate for column 2 - phase I (using 50 mM citrate) is thus similar to the value determined at the Hanford site. The citrate degradation rates for column 1 and column 2 - phase II were two orders of magnitude higher than that for column 2 - phase I. This suggests that the citrate degradation kinetics may also be dependent on the citrate concentration.

Assuming that the decreases in Ca and P concentrations in the columns were due to the precipitation of calcium phosphate (apatite), the amounts of apatite formed within the columns were calculated from the differences in the concentrations of Ca and P between the influent and effluent ends and the cumulative flux of the solution that had passed through the columns. The amounts of apatite were calculated to be 0.475, 1.140, and 0.194 mg apatite/g sediment for column 1, column 2 - phase I, and column 2 - phase II, respectively. Assuming 11 % of substitution of Sr for Ca in the structure of apatite (Szecsody et al., 2007) and 15 m thick apatite barrier, and with the given values of concentration of Sr in the site groundwater (0.06 mg/L), ground-

water velocity (0.3 m/day), porosity of sediment (0.36), and bulk density (1.5 g/cm^3), it is calculated that 300 yrs of treatment (10 times of half-life of Sr-90) will require 0.72 mg apatite/g sediment. This indicates that although the majority of calcium and phosphate did not precipitate within the column, some amounts of apatite comparable to the treatment for 300 yrs for the field site could be achievable under the column conditions.

The column operation conditions (i.e., continuous supply of the source solution) may be different than the conditions of the field injection (i.e., one time injection or multiple short-time injections). Other factors to consider include: 1) groundwater flow rate is faster in the column than the field conditions, 2) apatite precipitation rate is slow (i.e., kinetic limitation), and 3) calcium forms complexes with citrate degradation products. It is expected that in the field conditions, citrate degradation products will eventually be degraded and the injected calcium and phosphate will be precipitated as apatite in the long-term.

The amount of Sr sorbed on the sediment/apatite during phase III of column 2 was calculated to be 0.0236 mg Sr/g sediment/apatite, based on the Sr concentration profiles and the cumulative water flux. It is known that apatite minerals are very stable in water; the solubility product of hydroxy-

apatite is about 10^{-44} (Verbeeck et al., 1977). In the short term, the precipitate formed in the conditions similar to this study is amorphous and poorly crystalline monocalcium phosphate (Moore et al., 2004; Vermeul et al., 2014). The formation of amorphous and poorly crystalline monocalcium phosphate occurs within a week, while crystalline apatite forms within a few weeks (Vermeul et al., 2014). Therefore, the migration of the Sr concentration profile may be due to the dissolution of amorphous calcium phosphate upon supply of the groundwater with low ionic strength. It warrants further tests regarding the long-term functionality of crystallized apatite after a few months of the column experiments.

4. Conclusions

To evaluate the applicability of the injectable apatite sequestration method for Sr-90, laboratory column experiments were conducted. The columns were tested to evaluate the biodegradation of citrate, the formation of calcium phosphate (apatite), and the treatability of strontium by the sediment and apatite. The results indicate that the citrate is degraded, forming acetate and formate. However, the initially-formed calcium phosphate solid may be partially dissolving due to the changes in the geochemical conditions. The results also suggest that complexation of calcium with citrate degradation products may be occurring and apatite precipitation may be kinetically limited. Although the majority of calcium and phosphate was not precipitated within the columns, the calculations indicate that some amounts of calcium phosphate solid were formed under the column conditions. The calculated citrate degradation rates were 1.108, 0.013, and 2.134 hr^{-1} for column 1, column 2 - phase I, and column 2 - phase II, respectively, corresponding to the half-lives of 0.626, 53.319, and 0.325 hr, respectively. The citrate degradation rate for column 2 - phase I (using 50 mM citrate) is similar to the value determined in the previous study, while the rates for column 1 and column 2 - phase II are two orders of magnitude higher.

The treatability test, using the site groundwater spiked with stable Sr, determined whether or not Sr can be treated with the sediment and apatite formed. The results showed that the Sr was completely treated within 5-15 cm from the influent end. The migration of the Sr treatment front may be due to either exhaustion of sorption capacity of sediment/apatite or dissolution of amorphous calcium phosphate that was previously formed. This study provides a fundamental understanding of reaction mechanisms underlying the injectable apatite sequestration method for Sr-90 removal.

Acknowledgements

References

Chang, H.-S., Um, W., Rod, K., Serne, R.J., Thompson, A., Perdrial, N., Steefel, C.I., and Chorover, J., 2011, Strontium and cesium release mechanisms during unsaturated flow through waste-weathered Hanford sediments. *Environ. Sci. Technol.*, **45**, 8313-8320.

Fritz, B.G., Vermeul, V.R., Fruchter, J.S., Szecsody, J.E., and Williams, M.D., 2011, 100-NR-2 Apatite Treatability Test: An Update on Barrier Performance. PNNL-20252. Pacific Northwest National Laboratory, Richland, Washington, May 2011.

Hughes, J.M., Cameron, M., and Crowley, K.D., 1989, Structural variations in natural F, OH and Cl apatites. *Am. Mineral.*, **74**, 870-876.

Killey, R.W.D. and Munch, J.H., 1987, Radiostrontium migration from a 1953-54 liquid release to a sand aquifer. *Water Poll. Res. J. Canada*, **22**, 107-128.

Mehlich, A., 1938, Use of triethanolamine acetate-barium hydroxide buffer for the determination of some base exchange properties and lime requirement of soil. *Soil Sci. Soc. Am. Proc.* **29**, 374-378.

Moore, R.C., Sanchez, C., Holt, K., Zhang, P., Xu, H., and Choppin, G.R., 2004, Formation of hydroxyapatite in soils using calcium citrate and sodium phosphate for control of strontium migration. *Radiochimica Acta*, **92**, 719-723.

Rabideau, A.J., Benschoten, J.V., Patel, A., and Bandilla, K., 2005, Performance assessment of a zeolite treatment wall for removing Sr-90 from groundwater. *J. Contam. Hydrol.*, **79**, 1-24.

Seneca, S.M. and Rabideau, A.J., 2013, Natural zeolite permeable treatment wall for removing Sr-90 from groundwater. *Envi-*

ron. Sci. Technol., **47**, 1550-1556.

Spence, R.D. and Shi, C., 2005, Stabilization and Solidification of Hazardous, Radioactive, and Mixed Wastes. Boca Raton, Florida, CRC Press.

Szecsody, J.E., Burns, C.A., Moore, R.C., Fruchter, J.S., Vermeul, V.R., Williams, M.D., Girvin, D.C., McKinley, J.P., Truex, M.J., and Phillips, J.L., 2007, Hanford 100-N Area Apatite Emplacement: Laboratory Results of Ca-Citrate-PO₄ Solution Injection and Sr-90 Immobilization in 100-N Sediments. PNNL-16891. Pacific Northwest National Laboratory, Richland, Washington, September 2007.

Szecsody, J.E., Vermeul, V.R., Fruchter, J.S., Williams, M.D., Rockhold, M.L., Qafoku, N.P., and Phillips, J.L., 2010, Hanford 100-N Area In Situ Apatite and Phosphate Emplacement by Groundwater and Jet Injection: Geochemical and Physical Core Analysis. PNNL-19524. Pacific Northwest National Laboratory, Richland, Washington, July 2010.

Thompson, K.M., Fabre, R.J., Szecsody, J., Vermeul, V., Fellows, R., Williams, M., and Fruchter, J., 2009, An Innovative Approach for Constructing an In Situ Barrier for Strontium-90 at the Hanford Site, Washington. *Waste Management 2009*, Phoenix, Arizona.

Vermeul, V.R., Szecsody, J.E., Fritz, B.G., Williams, M.D., Moore, R.C., and Fruchter, J.S., 2014, An injectable apatite permeable reactive barrier for in situ ⁹⁰Sr immobilization. *Ground Water Monit. R.*, **34**(2), 28-41.

Verbeeck, R.M.H., Hauben, M., Thun, H.P., and Verbeeck, F., 1977, Solubility and solution behavior of strontium hydroxyapatite. *Z. Phys. Chem.* (Wiesbaden), **108**(2), 203-215.

Williams, M.D., Fritz, B.G., Mendoza, D.P., Rockhold, M.L., Thorne, P.D., Xie, Y., Bjornstad, B.N., Mackley, R.D., Newcomer, D.R., Szecsody, J.E., and Vermeul, V.R., 2008, Interim Report: 100-NR-2 Apatite Treatability Test: Low-Concentration Calcium-Citrate-Phosphate Solution Injection for In Situ Strontium-90 Immobilization. PNNL-17429, Pacific Northwest National Laboratory, Richland, Washington, July 20008.

Yin, J., Jeen, S.-W., Lee, D.R., and Mayer, K.U., 2014, Reactive transport modeling of ⁹⁰Sr sorption in reactive sandpacks. *J. Hazard. Mater.*, **280**, 685-695.